

M.K. Cheng, J.C. Ries, and B.D. Tapley

Abstract

The Earth's center of mass (CM) is defined in the satellite orbit dynamics as the center of mass of the entire Earth system, including the solid earth, oceans, cryosphere and atmosphere. Satellite Laser Ranging (SLR) provides accurate and unambiguous range measurements to geodetic satellites to determine variations in the vector from the origin of the ITRF to the CM. Estimates of the Global mass redistribution induced geocenter variations at seasonal scales from SLR are in good agreement with the results from the global inversion from the displacements of the dense network of GPS sites and from ocean bottom pressure model and GRACE-derived geoid changes.

Keywords

Geocenter • Satellite laser ranging (SLR) • Center of mass

1 Introduction

The Terrestrial Reference System (TRS) is a fundamental concept for all studies in the geosciences, and it is of critical importance for satellite navigation and other geoinformation applications. The Earth's center of mass (CM or geocenter) is the center of mass of the entire Earth system, including the solid earth, oceans, cryosphere surface water and atmosphere. The CM is the point about which any Earth satellite will orbit and can be determined from observations of an Earth-orbiting satellite motion. The origin of the International Terrestrial Reference Frame (ITRF) is currently derived from long-term analysis of Satellite Laser Ranging (SLR) data, but its dynamic tie to the CM is not yet a component of the conventional model of ITRF. The variation of the CM with respect to the origin of ITRF is known as the geocenter motion and reflects the global scale mass redistribution and the interaction between the solid Earth and the mass loading. Determination of the Earth's center of mass is

an important component for the realization of the Terrestrial Reference System, and has attracted considerable attention; see for example Trupin et al. (1992), Dong et al. (1997), Watkins and Eanes (1997), Pavlis (2002), Angermann and Müller (2008), Pavlis and Kusmierz-Cieslak (2009), and those papers that contributed to the *IERS Analysis Campaign to Investigate Motions of Geocenter* (Ray 1999).

In this study, the geocenter motion is simultaneously estimated along with the low-degree portion of the gravity field, providing a unified recovery of the signals in the SLR data. This paper discusses the analysis of estimates of the annual geocenter variations from a multi-satellite SLR data set and compares the results with the ILRS SLR network translation solutions (Collilieux et al. 2009; Altamimi et al. 2010) based on the International Laser Ranging Service (ILRS; Pearlman et al. 2002) and the global inversion mostly based on the 3-dimensional displacement of GPS stations (Wu et al. 2010a).

2 Theory

The Earth's gravitational potential is expressed by a spherical harmonic with coefficients (C_{nm} and S_{nm}), which are a function of the global mass distribution determined by a volume

M.K. Cheng (✉) • J.C. Ries • B.D. Tapley
Center for Space Research, University of Texas at Austin, Austin,
TX 78759-5321, USA
e-mail: cheng@csr.utexas.edu

integral enveloping the entire Earth system (see Heiskanen and Moritz 1967; Torge 1980; Lambeck 1988). By definition, the coordinates of the CM in the adopted reference system are determined by the degree-one normalized spherical harmonic coefficients C_{10} , C_{11} and S_{11} . The geocenter vector from origin of the reference system to the mass center is given by

$$\vec{r}_{cm} = a_e \sqrt{3} (C_{11}, S_{11}, C_{10}) \quad (4.1)$$

where a_e is the Earth's radius.

In a reference frame centered exactly at the CM, the degree-one harmonics are identically zero. The origin of the geocentric inertial reference frame, for high accuracy satellite orbit determination, is typically chosen to coincide with the CM, and the geocenter vector \vec{r}_{cm} represents the offset between the ITRF origin and the instantaneous CM. As an alternate, a geocentric frame at the ITRF origin can be used, but in this case the degree-one terms are non-zero. However, it is also necessary for proper modeling to include a Coriolis-type force due to the fact that the origin is no longer an inertial reference point (Kar 1997).

The geocenter vector \vec{r}_{cm} can be determined using space geodetic measurements, which link a satellite (which orbits about the center of mass of the Earth system) and the tracking sites (which realize the origin of the crust-fixed International Terrestrial Reference Frame (ITRF)) based on the geometric relation:

$$\vec{r}(t) = \vec{\rho}(t) + \vec{R}_{sj} - \vec{r}_{cm}(t) \quad (4.2)$$

where \vec{r} is the position vector of the satellite related to the Earth's mass center and determined by integrating Newton's equations in a non-rotating geocentric reference frame, $\vec{\rho}$ is the range vector from the tracking site to the satellite. The vector \vec{r} and $\vec{\rho}$ are expressed in the earth-body-fixed system. \vec{R}_{sj} is the position vector of a tracking site with respect to the ITRF. \vec{r}_{cm} is the vector from the origin of the ITRF to the CM (identical to the vector O_G described in the IERS conventions (McCarthy and Petit 2003; Petit and Luzum 2010)). Global mass redistribution alters Earth rotation, produces temporal variations of the gravitational field, and variations of the CM with respect to the origin of ITRF (as convention, the origin of ITRF is fixed to the crust of the Earth). This variation is referred to as geocenter motion.

The Earth consist of the solid and fluid layer, the volume integral over the entire Earth for the degree one spherical harmonic coefficients can be expressed mathematically as the sum of the volume integral for the solid earth and a shell integral for fluid thin layer (with thickness much less than a_e), which depends on the mass distribution and variable boundary as the deformable earth surface in response to mass loading. Let $\Delta\sigma(\phi, \lambda)$ be the change in the surface density (mass/area) as radial integral of the density

distribution through the thin layer (Eq. (5) of Wahr et al. 1998). Thus, the mass loading of the thin layer induced normalized coefficients C_{10}^f , C_{11}^f , S_{11}^f are determined by the surface integral of density changes $\Delta\sigma(\phi, \lambda)$ taken over the Earth's fluid surface thin layer with the surface element dS as follows (Chao et al. 1987, Eq. (6) of Wahr et al 1998):

$$C_{10}^f = \frac{a_e^2}{3M} \iint_{E_s} \Delta\sigma(\phi, \lambda) \sin \phi dS \quad (4.3)$$

$$C_{11}^f = \frac{a_e^2}{3M} \iint_{E_s} \Delta\sigma(\phi, \lambda) \cos \phi \cos \lambda dS \quad (4.4)$$

$$S_{11}^f = \frac{a_e^2}{3M} \iint_{E_s} \Delta\sigma(\phi, \lambda) \cos \phi \sin \lambda dS \quad (4.5)$$

Correspondingly, the geocenter vector can be expressed as $\vec{r}_{cm} = \vec{r}_{cm}^s + \vec{r}_{cm}^f$. The vector \vec{r}_{cm}^s represents the coordinate of the center of mass of the solid Earth without the fluid load and deformation, evaluated by the volume integral for the solid earth assuming the mass of the solid earth approximates to the mass of whole Earth. The vector \vec{r}_{cm}^f represents the coordinate of the center of the fluid thin surface layer, within which the mass is free to be redistributed (Blewitt 2003). \vec{r}_{cm}^f is evaluated by the mass loading of the thin layer (described by C_{10}^f , C_{11}^f , S_{11}^f) and loading induced deformation of the earth surface (Eq. (7) of Wahr et al. 1998). Both vectors, \vec{r}_{cm}^s and \vec{r}_{cm}^f , are with respect to the origin of the selected reference frame (ITRF). Unfortunately, \vec{r}_{cm}^s is not directly observable from crust-based observations while the modeling of \vec{r}_{cm}^f is uncertain. However, \vec{r}_{cm} (the sum of \vec{r}_{cm}^s and \vec{r}_{cm}^f) is observable from analysis of SLR data.

The evaluation of \vec{r}_{cm}^f has been a principal concern in the past because of the complexity of the density redistribution and variable boundary surface, which covers the solid earth and separates from the fluid thin layer. In the earlier study, such as Trupin et al. (1992) and Dong et al. (1997), \vec{r}_{cm}^f referred to the center of figure of the "outer surface of the solid Earth". This surface is assumed to be covered by a uniform infinitely dense array of points and the motions of these points are taken into account (Blewitt 2003), but this is very difficult to realize in practice (Dong et al. 2003). Even the current dense global GPS network represents only a portion of the surface of the solid Earth.

In recent developments, \vec{r}_{cm}^f is evaluated by the 'thin-shell loading model' (Blewitt 2003). In this model, the boundary is defined by a sphere of radius a_e used for the approximate spherical harmonic expansion of the density variations (Eq. (9) of Wahr et al. 1998). The normalized spherical harmonic coefficients (denoted as C_{lm}^σ and S_{lm}^σ) can be

inferred from a global inversion based on the GPS-determined three-dimensional displacements for a global dense network and the ocean bottom pressure (OBP) model along with the GRACE-derived geoid changes (Wu et al. 2006, 2010a,b). Thus, the notation of CF is still used for \vec{r}_{cm}^f from the ‘thin-shell loading model’, which better represents \vec{r}_{cm}^f than the earlier studies.

The variations of \vec{r}_{cm} are determined by the time varying density distribution within the Earth system as the response of the Earth to the movements of the planetary fluid masses and the crustal movements due to tectonic motion and earthquakes. Among these variations, the changes of \vec{r}_{cm}^f are mostly due to the climate change induced movements of the planetary fluid masses and surface displacement in response to the changes of the loading on the Earth’s surface. In the frequency domain, the vector \vec{r}_{cm}^s is relatively static with variations only on geological time scales; \vec{r}_{cm}^f describes the variations with time scales from sub-daily to seasonal and longer. In the past decades, considerable efforts were made to determine the changes of \vec{r}_{cm}^f by estimating or modeling the distribution of the mass density changes, $\Delta\sigma(\phi, \lambda)$, which can be represented by the equivalent water height (Wahr et al. 1998).

Center of the surface loading. For an elastic Earth, the thin fluid layer produces a gravitational (load) potential at the Earth’s surface, and resulting in surface displacements (deformation). The surface displacement further produces additional potential change (Lambeck 1988) based on the load Love number theory. Thus, the vector of the surface loading center \vec{r}_{cm}^L can be determined by the degree one terms in the surface density change induced potential (load plus additional potential from the loading induced deformation) based on the models of the redistributions of the atmosphere surface pressure, hydrosphere (soil moisture and water storage) and ocean mass (Dong et al. 1997; Chen et al. 1999) and ice melting.

Center of the fluid shell and global inversion. The coefficients \vec{r}_{cm}^L can be expressed in terms of the degree-one spherical harmonic coefficients of the surface density anomaly: C_{1m}^σ and S_{1m}^σ ($m = 0, 1$) ($m = 0, 1$) accounting for the surface mass loading induced potential (Eq. (12) of Wahr et al. 1998). Thus, \vec{r}_{cm}^f is determined from

$$\vec{r}_{cm}^f = \frac{a_e \rho_w}{\rho_e} (1 + k'_1) \sqrt{3} (C_{11}^\sigma, S_{11}^\sigma, C_{10}^\sigma) \quad (4.6)$$

where ρ_e and ρ_w are the mean density of the solid earth and water, respectively. k'_1 is the degree-one load Love number for an elastic lithosphere (Farrell 1972). In the frame associated with the center of mass of just the solid earth (CE), $(1 + k'_1) = 1$. This relation can be applied to the estimates of geocenter variations from global inversion assuming the center of figure of the GPS network (CF) and CE are approximately equivalent (Blewitt 2003; Jansen et al. 2006).

The response of the solid Earth surface to loading changes caused by mass redistribution in the thin surface layer is the displacement in the local vertical and horizontal directions. Those displacements are proportional to the load potential and the gradient of the load potential characterized by the load Love number (Lambeck 1988). They can be expressed in terms of the spherical harmonic coefficients of the surface density changes (or anomalies) based on Farrell’s (1972) loading theory.

Thus, the three dimensional displacement vectors of the GPS network (combined with the observed geoid changes from GRACE measurements or OBP models) were used to infer the degree-one terms of the loading density distribution to obtain the estimates of \vec{r}_{cm}^f . This method is described as a global inversion (Blewitt and Clarke 2003; Wu et al. 2003; Kusche and Schrama 2005; Jansen et al. 2009; Wu et al. 2010a). The surface density changes observed from GRACE were used to determine the induced geoid changes in the global inversion to improve separation of the information related to the degree-one terms in the observed displacements from GPS data analysis, and can be used to determine the loading displacement of tracking stations due to the loading potential except for the degree-one terms.

3 Determining Geocenter from SLR

Among the space geodetic techniques, the difficulty in modeling of the nongravitational forces acting on satellites limits the ability of the GPS and DORIS techniques to accurately measure the geocenter vector \vec{r}_{cm} . Satellite laser ranging (SLR) is currently the best means of obtaining precise and unambiguous range measurements for the various passive geodetic satellites, and this accurate range information allows the determination of even very small gravitational forces acting on them. The SLR data has, over the past three decades, provided long-term, stable determinations of the origin of the ITRF. The geocenter motion is usually not modeled in the precise orbit determination for SLR data analysis, and this signal will remain in the residuals.

The geocenter vector \vec{r}_{cm} is defined geometrically in the observation equation assuming the coordinates of the tracking stations are described by the ITRF system. Conventional (pre-GRACE) gravity models were obtained assuming the CM coincides with the origin of the ITRF used for the tracking station coordinates. Consequently, the offset of the origin of the ITRF from the CM could be aliased into the geopotential coefficients estimated from space geodetic measurements. This will not occur with GRACE-based models, since the GRACE inter-satellite range data is insensitive to the geocenter motion. In the approach used in this study,

the geocenter motion is estimated simultaneously with the orbit, force and measurement parameters from the SLR data.

In order to study the station displacements and the realization of the ITRF, an alternative approach is commonly used. Instead of directly estimating the geocenter motion \vec{r}_{cm} , the station displacements $\Delta\vec{R}_{sj}$ ($j = 1, N$) are estimated for the entire SLR network (with $N = \sim 20\text{--}30$ over 1 month intervals) along with the estimation of a number of (constant or once-per-rev) empirical acceleration parameters. The estimated network station coordinates ($\vec{R}_{sj} + \Delta\vec{R}_{sj}$) are then projected into the ITRF by a Helmert transformation defined by seven parameters: three translation parameters, one scale and three coordinate rotation angles. The translation reflects the origin difference between the estimated displaced station network and the ITRF used in the analysis, for which the origin is not necessarily the CM, at least at the seasonal and shorter time scales (Dong et al. 2003). This approach is used by the ILRS and earlier analyses from SLR (e.g., Eanes et al. 1997). A concern with this approach is that the orbit may have accommodated some of the geocenter motion, particularly in the Z direction, and thus may have attenuated the geocenter variation in that component.

As noted previously, a gravity field including the degree-one geopotential coefficients can be obtained using the space geodetic tracking data by fixing the tracking station coordinates to the ITRF. This is equivalent to the estimation of the geocenter motion (\vec{r}_{cm}) along with the geopotential coefficients with degree greater than one in this study, though a completely correct modeling requires the addition of Coriolis-type terms with the former approach. Simultaneously estimating the degree-one coefficients and the entire network displacements would be ill conditioned because they are equivalent and determined using the same observation information.

The satellites used in this study (Starlette, Ajisai, Stella, LAGEOS-1 and LAGEOS-2) all have spherical shapes, which simplifies the modeling of the non-gravitational forces. In addition, except for Ajisai, they have dense metal cores and very low area-to-mass ratios, which further reduces the impact of the non-gravitational force modeling errors. The orbit inclination ranges from 50° to 109° , and the altitudes range from 700 to 6,000 km. To accommodate residual dynamic modeling errors, 12-h drag coefficients (C_D) or empirical along-track acceleration parameters (C_T) were conventionally estimated as part of the precision orbit determination process. While these parameters have the potential to affect the determination of the gravitational forces, they are essential to accommodate the residual errors in the surface force modeling.

The background gravity models, such as the solid earth and ocean pole tides as well as the atmosphere and ocean de-aliasing (AOD) employed in this analysis are generally consistent with those for the GRACE RL04 products

(Bettadpur 2007). The station displacement due to solid earth tides and ocean loading are modeled based on the IERS 2003 conventions, including the effects due to the diurnal and semidiurnal tidally-induced geocenter variations (Watkins and Eanes 1997). The station coordinates are based on LPOD2005 (Ries 2008), which is consistent with ITRF2005 but with some additional stations, coordinate updates and range bias modeling. To measure the geocenter signal at the mm level, this study used a short arc orbit analysis with an arc length of 3 days for the monthly solutions and 7 days for the weekly solutions.

Two SLR time series were obtained in this study. The first (SLR-w) consists of weekly solutions for the geopotential coefficients (to degree and order 5) and the geocenter parameters spanning 18 years from November 1992 to December 2010. The EGM08 gravity model (Pavlis et al. 2008) was used without the AOD model to determine the weekly solutions that is consistent with models used by the ILRS Analysis Working Group (AWG). The second SLR time series (SLR-m) consists of 106 monthly solutions from five geodetic satellites over the period from January 2002 to October 2010. The AOD model was used in this case for consistency with the GRACE RL04 processing. Three components of the geocenter motion, \vec{r}_{cm} , are directly estimated along with other dynamical parameters, including the satellite state vector (weekly or 3 days for monthly), 12-h C_D (or C_T) and the lower portion of the gravity field up to degree 5, over time intervals from weekly to monthly (Cheng et al. 2011). The station positions are fixed and range biases are based on LPOD2005. This approach provides a unified recovery of the gravity signals in the SLR data. The C_{20} estimates from this series are used to replace the GRACE estimates for supporting the GRACE applications in extracting the mass variation signal in the hydrological, ocean and polar ice sheets (Cheng and Ries 2009).

Figures 4.1, 4.2 and 4.3 show the monthly estimates for the three components of the geocenter variation, as well as the seasonal and linear trends. Figures 4.4, 4.5 and 4.6 show the weekly estimates, along with the seasonal, linear and long-period variations. The SLR estimates of the geocenter motion \vec{r}_{cm} reflect the weekly or monthly averaged integrated effects of the crustal deformation due to global-scale mass exchange between the Earth components. The mean of the estimates for \vec{r}_{cm} represents the mean position of the geocenter in the ITRF as determined by the constant parts of the mass distribution of the entire Earth, which is dominated by \vec{r}_{cm}^s . Seasonal changes of the \vec{r}_{cm} about the mean correspond to the \vec{r}_{cm}^f , but could contain the information of the seasonal surface loading displacement of site positions due to the variations of the terms with degree greater than one in a spherical harmonic expansion of density variations. The effects for height displacement was discussed by van Dam et al. (2007). Further study is required

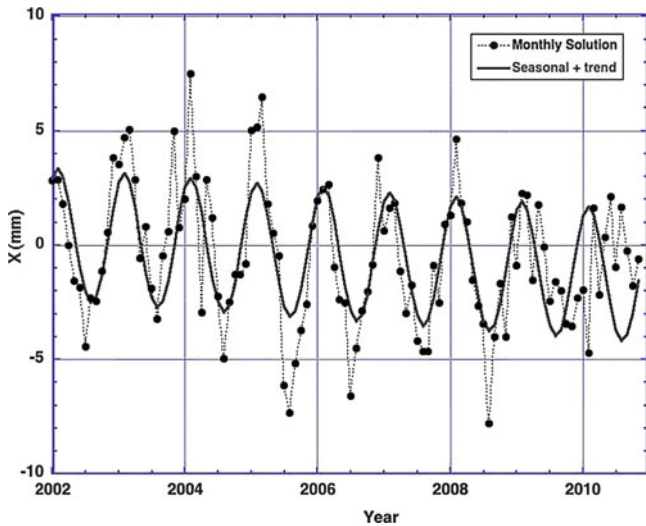


Fig. 4.1 Monthly geocenter variations in the X component. Linear + seasonal variation also shown

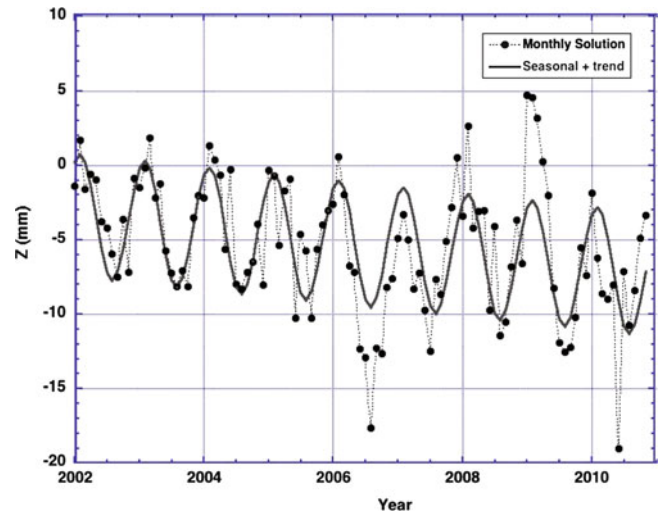


Fig. 4.3 Monthly geocenter variations in the Z component

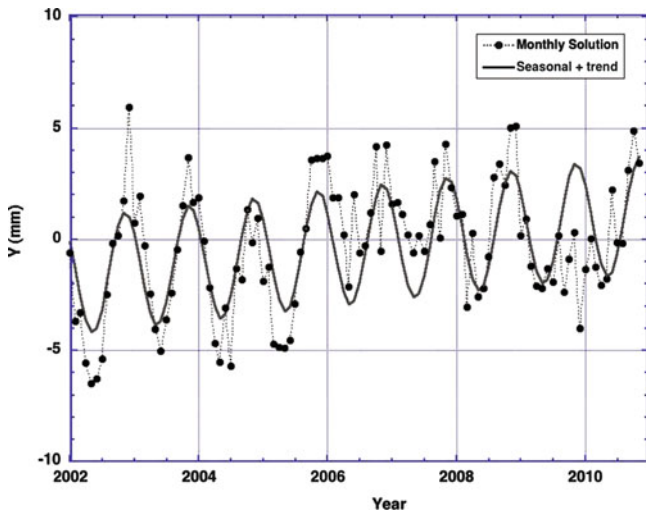


Fig. 4.2 Monthly geocenter variations in the Y component

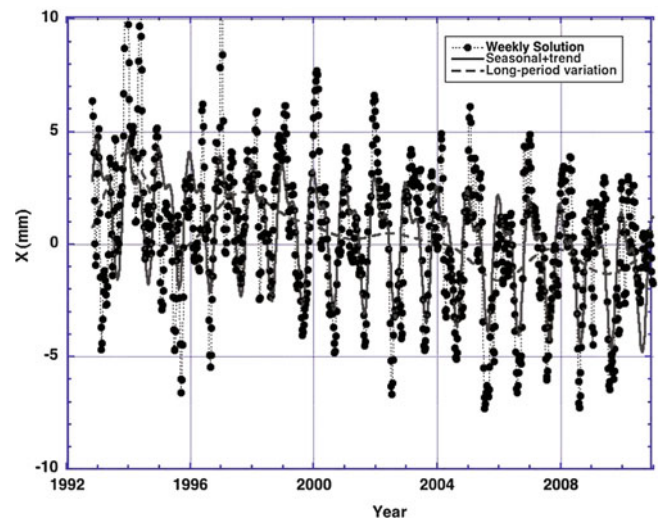


Fig. 4.4 Weekly geocenter variations in the X component. Seasonal + trend and long-period variations also shown

for evaluating these effects to correctly interpret the SLR-determined geocenter motion in comparison with the geophysical loading models and from the global inversion. While the loading surface mass change is expressed in a series spherical harmonics, the degree-one terms are directly related to the seasonal geocenter variations.

4 Comparison and Discussion

Table 4.1 compares the amplitude and phase for the annual variation of the geocenter motion from weekly (SLR-w) and monthly (SLR-m) solutions from this study, and the translation components estimated (with scale factor) from the 14-year weekly site position (denoted as ILRS-1) from the ILRS

AWG reported by Collilieux et al., (2009), and that estimated from analysis of 26 years of weekly site positions (denoted as ILRS-2) in the development of ITRF2008 (Altamimi et al. 2010). The notation of ‘Degree-one’ refers to the geocenter variation converted from the degree-one terms estimated from the global inversion based on the GPS/OBP/GRACE (Wu et al. 2010), where the effects above degree-one are based on the time series of the GRACE derived-gravity fields and OBP model.

Table 4.1 shows that the weekly solution from this study is in good agreement with the ILRS-2 solution for the three translation components. The agreement with ILRS-1 is not quite as good for Y (ILRS-1 amplitude is larger) or Z (ILRS-1 is smaller). The monthly SLR solution is in good

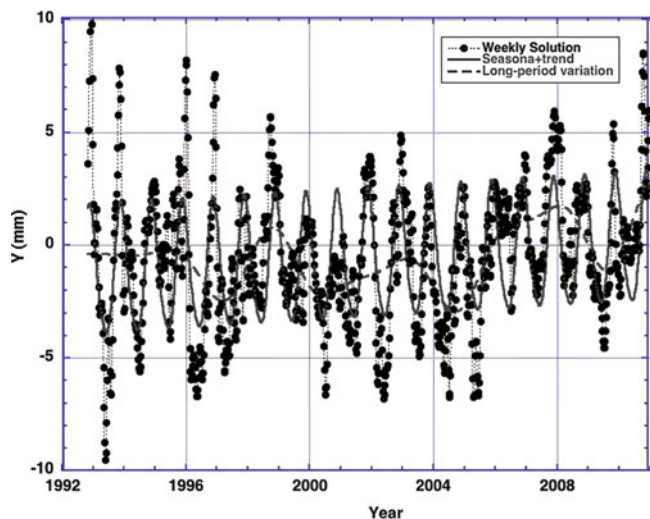


Fig. 4.5 Weekly geocenter variations in the Y component

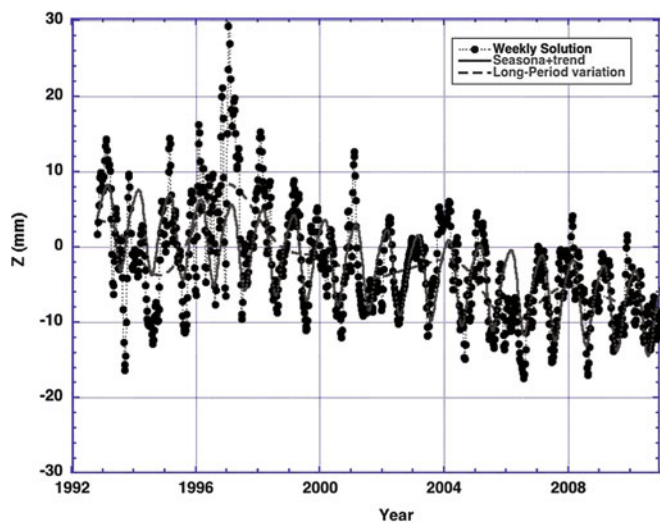


Fig. 4.6 Weekly geocenter variations in the Z component

agreement with the degree-one variations from the global inversion for the Y and Z component. The disagreement in X could be due to the network effect caused by an inadequate geographic distribution of SLR stations (Collilieux et al. 2009), or the global inversion results may be underestimating the variation in X.

The mean offset of the geocenter at epoch 2005.0 with respect to ITRF2005 is estimated to be -0.2 , -0.7 and -4.8 mm for X, Y and Z components, respectively, from this analysis. It is reasonably consistent with the estimates (-0.5 , 0.9 , and -4.7 mm) from ITRF2008 (Altamimi et al. 2010). The translation rate difference between ITRF2008 and ITRF2005 is reported to be zero for Y and Z, and 0.3 mm/y for X (± 0.2 mm/year for each) (Altamimi et al. 2010). However, drifts appear in the time series for all three

Table 4.1 Observed geocenter variations (amplitude in mm; phase in degrees). Error estimates are formal errors only. Convention is Amp cos ($\omega(t-t_0)$ -Phase) where t_0 is January 1

Case	X (Amp/Phase)	Y (Amp/Phase)	Z (Amp/Phase)
SLR-w	$2.7 \pm 0.2/$ 40 ± 2	$2.8 \pm 0.2/$ 323 ± 2	$5.2 \pm 0.2/30 \pm 3$
ILRS-1	$2.7 \pm 0.3/$ 45 ± 4	$3.8 \pm 0.2/$ 327 ± 4	$3.6 \pm 0.4/4 \pm 7$
ILRS-2	$2.6 \pm 0.1/$ 40 ± 3	$3.1 \pm 0.1/$ 315 ± 2	$5.5 \pm 0.3/$ 22 ± 10
SLR-m	$2.9 \pm 0.4/$ 35 ± 3	$2.6 \pm 0.2/$ 306 ± 2	$4.2 \pm 0.3/33 \pm 2$
Degree-one	$1.8 \pm 0.2/$ 49 ± 3	$2.7 \pm 0.2/$ 325 ± 3	$4.2 \pm 0.2/31 \pm 3$

components from this analysis, as shown in Figs. 4.1, 4.2, 4.3, 4.4, 4.5 and 4.6. The rates are estimated to be -0.2 , 0.3 and -0.5 mm/year for X, Y and Z, respectively, although the uncertainty in these trends is probably at the same level. It is interesting that there appear a good agreement with the rates for X and Y (-0.2 and 0.4 mm/year, respectively) estimated from the global inversion (Wu et al. 2010a, b), though the agreement is poor for Z (-0.9 mm/year). Ice melting and postglacial rebound could produce a secular geocenter velocity on the order of 1 mm/year (Greff-Lefftz 2000; Métivier et al. 2010), and further study is required to understand if these signals are geophysically meaningful.

A scale parameter is not estimated in this analysis since the length scale of the reference frame determined from SLR is only related to the velocity of light (for the ranging measurement reduction) and GM (the product of the gravitational constant G and the mass of the Earth), although accurate knowledge of the satellite center of mass offset is also critical (Ries 2007). The variations and trends in the translation and scale seen in other analyses may be due to position/velocity errors or unmodeled ranging biases (Coulot et al. 2009).

In summary, time series of geocenter motion were determined from analysis of SLR data from five geodetic satellites over a period of 18 years from Nov. 1992 to Dec. 2010 for weekly solutions, and a period of 9 years from 2002 through 2010 for monthly solutions. Results reveal significant seasonal and possible interannual variations in all three components (X, Y, Z) of the geocenter motion. The estimates of the annual variations are generally in good agreement from the various SLR analyses, as well as with the global inversion approach based on GPS/OBP/GRACE. Simultaneous estimation of geocenter motion and gravity field, the approach used here, can provide a unified recovery of the mass redistribution signals in the SLR data.

Acknowledgments This research was supported by NASA grants NNX08AE99E and JPL1368074.

References

- Altamimi Z, Collilieux X, Métivier L (2010) ITRF2008: an improved solution of the international terrestrial reference frame. *J Geodesy*. doi:[10.1007/s00190-011-04444-4](https://doi.org/10.1007/s00190-011-04444-4)
- Angermann D, Müller H (2008) On the strengths of SLR observations to realize the scale and origin of the terrestrial reference system. In: Sideris MG (ed) *Observing our changing earth: Proceedings of the 2007 IAG General Assembly*, vol 133, pp 21–29. Springer, Perugia, 2–13 July 2007
- Bettadpur S (2007) UTCSR level-2 processing standards document for level-2 product release 0004, GRACE 327-742, <ftp://podaac-ftp.jpl.nasa.gov/allData/grace/>
- Blewitt G (2003) Self-consistency in reference frames, geocenter definition, and surface loading of the solid Earth. *J Geophys Res* 108 (B2):2103. doi:[10.1029/2002JB002082](https://doi.org/10.1029/2002JB002082)
- Blewitt G, Clarke P (2003) Inversion of Earth's changing shape to weigh sea level in static equilibrium with surface mass redistribution. *J Geophys Res* 108(B6):2311. doi:[10.1029/2002JB002290](https://doi.org/10.1029/2002JB002290)
- Chao BF, O'Connor WP, Change ATC, Hall DY, Foster J (1987) Snow load effects on the Earth's rotation and Gravitational field, 1979–1985. *J Geophys Res* 92(B9):9415–9422
- Chen JL, Wilson CR, Eanes RJ, Nerem RS (1999) Geophysical interpretation of observed geocenter variations. *J Geophys Res* 104:2683–2690
- Cheng MK, Ries J (2009) Monthly estimates of C20 from 5 SLR satellites, GRACE Technical Note 05, ftp://podaac.jpl.nasa.gov/allData/grace/docs/TN-05_C20_SLR.txt
- Cheng M, Ries JC, Tapley BD (2011) Variations of the Earth's figure axis from satellite laser ranging and GRACE. *J Geophys Res* 116: B01409. doi:[10.1029/2010JB008085](https://doi.org/10.1029/2010JB008085)
- Collilieux X, Altamimi Z, Ray J, van Dam T, Wu X (2009) Effect of the satellite laser ranging network distribution on geocenter motion estimation. *J Geophys Res* 114:B04402. doi:[10.1029/2008JB005727](https://doi.org/10.1029/2008JB005727)
- Coulot D, Bériot Ph, Bonnefond P, Exertier P, Féraudy D, Laurain O, Deleflie F (2009) Satellite laser ranging biases and terrestrial reference frame scale factor, observing our changing earth. *Proceedings of the 2007 IAG general assembly*, vol 133, pp 39–46. Springer, IAG, Perugia, 2–13 July 2007
- Dong D, Dickey JO, Chao Y, Cheng MK (1997) Geocenter variations caused by atmosphere, ocean and surface ground water. *Geophys Res Lett* 24(15):1867–1870
- Dong D, Yunck T, Heflin M (2003) Origin of the international terrestrial reference frame. *J Geophys Res* 108:B42200. doi:[10.1029/2002JB002035](https://doi.org/10.1029/2002JB002035)
- Eanes RJ, Kar S, Bettadpur SV, Watkins MM (1997) Low-frequency geocenter motion determined from SLR tracking data. *Eos Trans AGU*, 78(46), Fall meeting, Supplementary, F156
- Farrell WE (1972) Deformation of the Earth by surface loading. *Rev Geophys Space Phys* 10:761–797
- Greff-Lefftz M (2000) Secular variation of the geocenter. *J Geophys Res* 105(B11):25685–25692
- Heiskanen WA, Moritz H (1967) *Physical geodesy*. W. H. Freeman and Co., San Francisco/London
- Jansen MJF, Kusche J, Schrama EJO (2006) Low-degrees load harmonics coefficients from combining GRACE, GPS time series and a priori dynamics. In: *Proceedings IAG symposium, 2006*
- Jansen MJF, Gunter BC, Kusche J (2009) The impact of GRACE, GPS and OBP data on estimates of global mass redistribution. *Geophys J Int* 177:1–13. doi:[10.1111/j.1356-246X.2008.04031x](https://doi.org/10.1111/j.1356-246X.2008.04031x)
- Kar S (1997) Long-period variations in the geocenter observed from laser tracking of multiple satellites, CSR report CSR-97-2, The University of Texas Center for Space Research, Mail stop R1000, Austin, TX
- Kusche J, Schrama E (2005) Surface mass redistribution inversion from global GPS: a unified observation model. *J Geophys Res* 110: B09409. doi:[10.1029/2004JB003556](https://doi.org/10.1029/2004JB003556)
- Lambeck K (1988) *Geophysical geodesy*. Clarendon, Oxford
- McCarthy DD, Petit G (2003) *IERS conventions (2003) IERS technical note no. 32*, International earth rotation and reference systems service. Frankfurt, Germany
- Métivier L, Greffitz-Lefftz M, Atamimi Z (2010) On secular geocenter motion: the impact of climate changes. *Earth Planet Sci Lett* 296 (3–4):360–366. doi:[10.1016/j.epsl.2010.05.021](https://doi.org/10.1016/j.epsl.2010.05.021)
- Pavlis EC (2002) Dynamical determination of origin and scale in the earth system from satellite laser ranging. In: Adam J, Schwarz K-P (eds) *Vistas for geodesy in the new millennium*. Springer, New York, pp 36–41
- Pavlis EC, Kuzmich-Cieslak M (2009) Geocenter motion: causes and modeling approaches. In: Schillack S (ed) *Proceedings of 16th international laser workshop*, Poznan pp 16–26
- Pavlis NK, Holmes SA, Kenyon SC, Factor JK (2008) An earth gravitational model to degree 2160: EGM2008, 2008 general assembly of the European geosciences union, Vienna, Austria
- Pearlman MR, Degnan JJ, Bosworth JM (2002) The International laser ranging service. *Adv Space Res* 30(2):135–143. doi:[10.1016/S0273-1177\(02\)00277-6](https://doi.org/10.1016/S0273-1177(02)00277-6)
- Petit G, Luzum B, IERS Conventions (2010) IERS technical note no. 36, international earth rotation and reference systems service. Frankfurt, Germany
- Ray J (ed) (1999) IERS analysis campaign to investigate motions of the geocenter, IERS technical note 25, Observatoire de Paris, Paris
- Ries J (2007) Satellite laser ranging and the terrestrial reference frame: principal sources of uncertainty in the determination of the scale. *Geophys Res Abst* 9:10809, EGU General Assembly, Vienna, 15–20 April 2007 [SRef-ID: 1607-7962/gra/EGU2007-A-10809]
- Ries J (2008) LPOD2005: a practical realization of ITRF2005 for SLR-based POD, Ocean Surface topography science team meeting, 10–12 Nov 2008, Nice, France; available at <ftp.csr.utexas.edu/pub/jason/models/coords>
- Torge W (1980) *Geodesy*, De Gruyter, New York
- Trupin AS, Meier MF, Wahr J (1992) Effects of melting glaciers on the Earth's rotation and gravitational field: 1965–1984. *Geophys J Int* 108:1–15
- van Dam T, Wahr JM, Lavallée D (2007) A comparison of annual vertical crustal displacements from GPS and gravity recovery and climate experiment (GRACE) over Europe. *J Geophys Res* 114: B04402. doi:[10.1029/2006JB004335](https://doi.org/10.1029/2006JB004335)
- Wahr J, Molenar M, Bryan F (1998) Time variability of the Earth's gravity field: hydrological and oceanic effects and their possible detection using GRACE. *J Geophys Res* 103(B12):30,205–30,229
- Watkins MM, Eanes RJ (1997) Observations of tidally coherent diurnal and semi-diurnal variations in the geocenter. *Geophys Res Lett* 24:2231–2234
- Wu X, Argus D, Heflin M, Ivins E, Webb F (2003) Site distribution and aliasing effects in the inversion for load coefficients and geocenter motion from GPS data. *Geophys Res Lett* 30(14):1742. doi:[10.1029/2003GL017546](https://doi.org/10.1029/2003GL017546)
- Wu X, Heflin M, Ivins E, Fukumori I (2006) Seasonal and interannual global surface mass variations from multisatellites geodetic data. *J Geophys Res* 111:B09401. doi:[10.1029/2005JB004100](https://doi.org/10.1029/2005JB004100)
- Wu X, Heflin M, Schotman H, Vermeersen B, Dong D, Gross R, Ivins E, Moore A, Owen S (2010a) Simultaneous estimation of global present-day water transport and glacial isostatic adjustment. *Nat Geosci*. doi:[10.1038/NCEO938](https://doi.org/10.1038/NCEO938)
- Wu X, Collilieux X, Altamimi Z (2010b) Data sets and inverse strategies for global surface mass variations. *Geophys Res Abst* 12, EGU2010-5484, <http://meetingorganizer.copernicus.org/EGU2010/EGU2010-5484.pdf>